Extension of the Transfer Matrix Method for Rotordynamic Analysis to Include a Direct Representation of Conical Sections and Trunnions

M. S. DARLOW
Consultant,
Mechanical Technology Inc.,
Latham, N. Y. 12110

B. T. MURPHY
Graduate Asst.,
Texas A & M University
College Station, Tex. 77843

J. A. ELDER
Student,
University of Florida
Gainesville, Fla. 32611

G. N. SANDOR
Research Professor,
Dept. of Mechanical Engineering,
University of Florida,
Gainesville, Fla. 32611

The transfer matrix method for rotordynamic analysis (alternately known as the HMP or LMP method) has enjoyed wide popularity due to its flexibility and ease of application. A number of computer programs are generally available which use this method in various forms to perform undamped critical speed, unbalance response, damped critical speed and stability analyses. For all of these analyses, the assembly of the transfer matrices from the rotor model is essentially the same. In all cases, the rotor model must be composed entirely of cylindrical beam elements. There are two situations when this limitation is not desirable. The first situation is when the rotor being modelled has one or more sections whose cross sections vary continually in the axial direction. The most common of these sections is the conical section. Presently, a conical section must be modelled as a series of "steps" of cylindrical sections. This adversely affects both the simplicity and accuracy of the rotor model. The second situation when current transfer matrix techniques are not accurate is when the rotor being modelled has one or more sections that do not behave as beam elements. The most common example is a trunnion which behaves as a plate. This paper describes the analytical basis and the method of application for direct representation of conical sections and trunnions for a transfer matrix analysis. Analytical results are currently being generated to demonstrate the need for and advantages of these modelling procedures.

Introduction

The most commonly used tools for rotordynamic analysis employ a transfer matrix representation, based on the works of Myklestad [1] and Prohl [2]. This is a linear analysis in which a rotor is treated as a series of beams. The original procedure, conceived independently by Myklestad and Prohl, is used to determine the undamped synchronous critical speeds of a rotor-bearing system. Subsequently, Lund [3, 4] adapted the procedure for calculating damped unbalance response and damped nonsynchronous natural frequencies and stability of a rotor with asymmetric supports. Lund has also expanded the transfer matrix analysis to handle multiple, interconnected rotors.

For all of these analytical tools, the rotor is represented by a series of uniform (cylindrical) beam elements. In most cases this is perfectly adequate and minor non-uniformities in the rotor (e.g., mild tapers) can be easily and accurately approximated by one or more uniform beam elements. However, there are certain rotor section shapes which are not easily modelled in this manner. Two such rotor section shapes are considered in this paper.

The first of these sections is, in the general case, where the cross-sectional moment of inertia and area vary continually in the axial direction. A set of integral equations are derived which represent the elements of the transfer matrix for this case. For the particular case of a conical section, which is the most frequently encountered non-uniform rotor section, these integral equations are solved in a closed-form for the elements of the transfer matrix. A damped critical speed computer program written by Vance [5], based on the work of Lund [4], is being modified to include this transfer matrix representation for a conical section. An analytical study is being performed to demonstrate the need for and advantages of using this conical section representation. Although the conical section is the only non-uniform rotor section for which an explicit solution is given in this paper, this approach is clearly applicable for any non-uniform rotor section for which these integral equations may be solved (analytically or numerically).

Some rotors have sections which do not behave like beams. In this case, the standard transfer matrix representation is totally inadequate. The most common rotor section of this type is the trunnion. A trunnion is essentially a circular plate, sup-

Contributed by the Vibrations Committee and presented at the Design Engineering Technical Conference, St. Louis, Mo., Sept. 10-12, 1979 of the American Society of Mechanical Engineers. Manuscript received at ASME Headquarters June 7, 1979. Paper No. 79-DET-58.

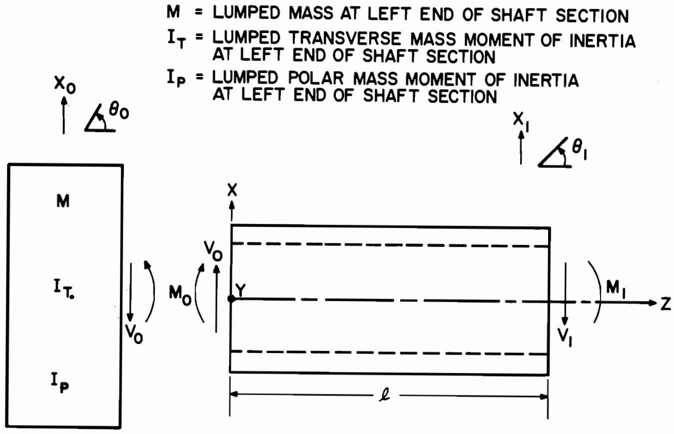

Fig. 1 Transfer Matrix Representation for a Uniform Shaft Section

ported around the periphery, and subjected to a central moment about a transverse axis. The angular stiffness of a trunnion is much less than that of a beam with similar dimensions. Using a theory of elasticity approach, an expression is derived for the angular stiffness of a trunnion with either a simply supported or a built-in edge. A transfer matrix representation is constructed, which accounts for the angular flexibility of the trunnion. Using the damped critical speed computer program mentioned above, modified to include the trunnion transfer matrix, an analytical study is being performed to demonstrate the need for and advantages of using this trunnion representation.

There are numerous practical situations in rotordynamic modelling where the use of conical section or trunnion representation would be very beneficial. The most outstanding cases are the rotating components of gas turbine engines. Specifically, compressor and turbine disks and overhanging branches often include both conical sections and trunnions. Similar cases may be found with steam turbines. Power transmission shafts often have conical sections, and occasionally have trunnions, integral with universal joint or coupling connections. Machines with rotating drums (i.e., hollow cylinders), such as ore tumblers, generally have a conical section or trunnion at one or both ends. These kinds of sections may also be found in compressors and other types of industrial machinery. Additionally, many machines have structural support components, often represented as outer shafts in rotordynamic analyses, which could be more accurately represented using conical sections or trunnions.

Standard Transfer Matrix

For the development of the standard transfer matrix, a uniform shaft section is considered, as shown in Fig. 1. The transfer matrix establishes the relationships of the radial displacement (x), slope (θ), bending moment (M), and shear force (V), at one end of the shaft section to the same quantities at the other end. Most existing transfer matrix analysis procedures [1, 2, 4] employ a lumped-mass model. That is, the shaft section is assumed to be massless and the appropriate mass is lumped at the ends of the shaft section. In general, this analysis may be conducted along orthogonal axes (e.g., X and Y). However, in each case the analysis is identical, with differences in notation only. Therefore, the development presented here is for the x-component, while it is clear that the equations for the y-component are analogous. The z direction is taken along the rotor bearing axis.

The bending equation for the shaft section is given by

$$M = EI\frac{d\theta}{dz} \tag{1}$$

where E (modulus of elasticity) and I (cross-sectional transverse moment of inertia) are invariant for a uniform shaft section, and θ is a function of z only. The bending moment, M, at any point along the shaft section may be represented in terms of the bending moment and shear force at $z = 0$ (M_0 and V_0), as shown in equation (2)

$$M = M_0 + V_0 z \tag{2}$$

Rearranging the terms in equation (1), substituting equation (2) and integrating, as shown in equation (3), results in equation (4)

$$\int d\theta = \frac{M_0}{EI}\int_0^z dz + \frac{V_0}{EI}\int_0^z z dz \tag{3}$$

$$\theta - C_1 = \frac{M_0}{EI} z + \frac{V_0}{EI}\frac{z^2}{2} \tag{4}$$

where C_1 is a constant of integration. By solving equation (4) for θ at $z = 0$ (which is known to be θ_0) C_1 is determined to be equal to θ_0. Consequently, θ is given by equation (5) and θ_1 (θ at $z=l$) is given by equation (6)

$$\theta = \frac{M_0 z}{EI} + \frac{V_0}{EI}\frac{z^2}{2} + \theta_0 \tag{5}$$

$$\theta_1 = \frac{M_0 l}{EI} + \frac{V_0 l^2}{2EI} + \theta_0 \tag{6}$$

where l is the length of the shaft section.

Including shear deformation, the rotation θ of the shaft section is related to the displacement x by

$$\theta = \frac{V_0}{\alpha GA} + \frac{dx}{dz} \tag{7}$$

where G (shear modulus), α (cross-sectional shape factor), and A (cross-sectional area) are invariant for a uniform shaft section, and x is a function of z only. Substituting equation (7) into equation (5) and rearranging terms gives

$$\frac{dx}{dz} = \frac{M_0}{EI} z + \frac{V_0}{EI}\frac{z^2}{2} + \theta_0 - \frac{V_0}{\alpha GA} \tag{8}$$

Multiplying through by dz and integrating both sides yields

$$x - C_2 = \frac{M_0}{EI}\frac{z^2}{2} + \frac{V_0}{EI}\frac{z^3}{6} + \theta_0 z - \frac{V_0}{\alpha GA} z \tag{9}$$

Letting z equal to zero in equation (9) reveals that C_2 (a constant of integration) must be equal to x_0. Thus, x is given by equation (10) and x_1 is given by equation (11)

$$x = \frac{M_0}{EI}\frac{z^2}{2} + \frac{V_0}{EI}\frac{z^3}{6} + \theta_0 z - \frac{V_0}{\alpha GA} z + x_0 \tag{10}$$

$$x_1 = \frac{M_0 l^2}{2EI} + V_0\left(\frac{l^3}{6EI} - \frac{l}{\alpha GA}\right) + \theta_0 l + x_0 \tag{11}$$

From equation (2), M_1 may be represented by

$$M_1 = M_0 + V_0 l \tag{12}$$

and V_1 is merely equal to V_0. The standard transfer matrix may then be assembled from equations (6), (11) and (12) to give

$$\begin{Bmatrix} x_1 \\ \theta_1 \\ M_1 \\ V_1 \end{Bmatrix} = \begin{bmatrix} 1 & l & \frac{l^2}{2EI} & \left(\frac{l^3}{6EI} - \frac{l}{\alpha GA}\right) \\ 0 & 1 & \frac{l}{EI} & \frac{l^2}{2EI} \\ 0 & 0 & 1 & l \\ 0 & 0 & 0 & 1 \end{bmatrix} \begin{Bmatrix} x_0 \\ \theta_0 \\ M_0 \\ V_0 \end{Bmatrix} \tag{13}$$

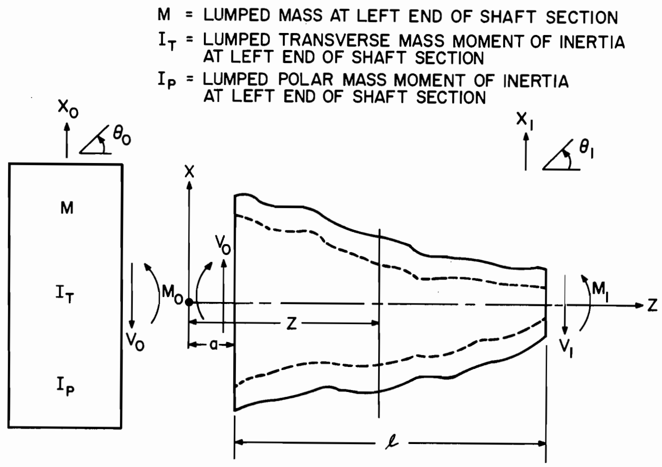

Fig. 2 Transfer Matrix Representation for a Non-Uniform Shaft Section

Transfer Matrix for Non-Uniform Shaft Section

A transfer matrix may be derived for a shaft section which is not uniform in the z-direction, shown in Fig. 2. In this case, equation (1) is replaced by

$$M = E(z)I(z)\frac{d\theta}{dz} \tag{14}$$

where the modulus of elasticity, E, and the cross-sectional moment of inertia, I, are functions of z. The bending moment, M, may still be represented by equation (2). However, equations (3) and (4) are replaced by equations (15) and (16)

$$\int d\theta = M_0\int_a^z \frac{dz}{E(z)I(z)} + V_0\int_a^z \frac{zdz}{E(z)I(z)} \tag{15}$$

$$\theta - C_3 = M_0\int_a^z \frac{dz}{E(z)I(z)} + V_0\int_a^z \frac{zdz}{E(z)I(z)} \tag{16}$$

where the values of E and I at the left end of the shaft section (see Fig. 2) are $E(a)$ and $I(a)$, respectively. The general value a is used to represent the left end of the shaft section, instead of zero, to ensure that the integrands are defined throughout the interval of integration. M_0, V_0, x_0 and θ_0 are the respective values at $z = a$.

For z equal to a, the integrals in equation (16) are equal to zero and C_3 (a constant of integration) must be equal to θ_0. Then, θ and θ_1 may be given by equations (17) and (18), respectively.

$$\theta = M_0\int_a^z \frac{dz}{E(z)I(z)} + V_0\int_a^z \frac{zdz}{E(z)I(z)} + \theta_0 \tag{17}$$

$$\theta_1 = M_0\int_a^{a+l} \frac{dz}{E(z)I(z)} + V_0\int_a^{a+l} \frac{zdz}{E(z)I(z)} + \theta_0 \tag{18}$$

Once expressions for $E(z)$ and $I(z)$ have been specified the integrals in equation (18) may be evaluated either analytically or numerically.

For a non-uniform shaft, equation (7) is replaced by

$$\theta = \frac{V_0}{\alpha(z)G(z)A(z)} + \frac{dx}{dz} \tag{19}$$

where the cross-sectional shape factor, α, the shear modulus, G, and the cross-sectional area, A, are functions of z. Substituting equation (19) into equation (17) and rearranging terms gives

$$\frac{dx}{dz} = M_0\int_a^z \frac{dz}{E(z)I(z)} + V_0\int_a^z \frac{zdz}{E(z)I(z)} - \frac{V_0}{\alpha(z)G(z)A(z)} + \theta_0 \tag{20}$$

Multiplying through by dz and integrating yields

$$x - C_4 = M_0\int_a^z\int_a^{z'} \frac{dzdz'}{E(z)I(z)} + V_0\int_a^z\int_a^{z'} \frac{zdzdz'}{E(z)I(z)} - V_0\int_a^z \frac{dz}{\alpha(z)G(z)A(z)} + \theta_0(z-a) \tag{21}$$

For z equal to a, the integrals in equation (21) are equal to zero and C_4 (a constant of integration) must be equal to x_0. Then, x and x_1 may be given by equation (22) and (23), respectively.

$$x = M_0\int_a^z\int_a^{z'} \frac{dzdz'}{E(z)I(z)} + V_0\int_a^z\int_a^{z'} \frac{zdzdz'}{E(z)I(z)} - V_0\int_a^z \frac{dz}{\alpha(z)G(z)A(z)} + \theta_0(z-a) + x_0 \tag{22}$$

$$x_1 = M_0\int_a^{a+l}\int_a^{z'} \frac{dzdz'}{E(z)I(z)} + V_0\int_a^{a+l}\int_a^{z'} \frac{zdzdz'}{E(z)I(z)} - V_0\int_a^{a+l} \frac{dz}{\alpha(z)G(z)A(z)} + \theta_0 l + x_0 \tag{23}$$

Equation (12) is still valid for M, and V_1 is again equal to V_0. The general transfer matrix for a non-uniform shaft section may then be assembled from equations (18), (23) and (12) to give

$$\begin{Bmatrix} x_1 \\ \theta_1 \\ M_1 \\ V_1 \end{Bmatrix} = \begin{bmatrix} 1 & l & k_4 & k_3 \\ 0 & 1 & k_1 & k_2 \\ 0 & 0 & 1 & l \\ 0 & 0 & 0 & 1 \end{bmatrix} \begin{Bmatrix} x_0 \\ \theta_0 \\ M_0 \\ V_0 \end{Bmatrix} \tag{24}$$

where

$$k_1 = \int_a^{a+l} \frac{dz}{E(z)I(z)} \tag{25}$$

$$k_2 = \int_a^{a+l} \frac{zdz}{E(z)I(z)} \tag{26}$$

$$k_3 = \int_a^{a+l}\int_a^{z'} \frac{zdzdz'}{E(z)I(z)} - \int_a^{a+l} \frac{dz}{\alpha(z)G(z)A(z)} \quad \text{(27) and}$$

$$k_4 = \int_a^{a+l}\int_a^{z'} \frac{dzdz'}{E(z)I(z)} \tag{28}$$

For E, I, α, G and A not functions of z, equations (24–28) reduce to equation (13) and k_2 is found to be equal to k_4. However, it should be noted that, in general, k_2 is not equal to k_4.

Once expressions for E, I, α, G and A as functions of z have been specified, the integrals in equations (25–28) may be evaluated either analytically or numerically and substituted into equation (24) for a transfer matrix analysis.

Conical Section Analysis

In this section, equations (25–28) are evaluated for the particular case of a conical section. The equations are also presented which are used for calculating the mass and transverse and polar mass-moments of inertia of a conical section for lumping at the ends of the rotor station.

For the purposes of this analysis, the expression for the cross-sectional moment of inertia, $I(z)$, of the conical section is simplified by assuming the section to have a thin wall. This approximation permits the closed form evaluation of all of the

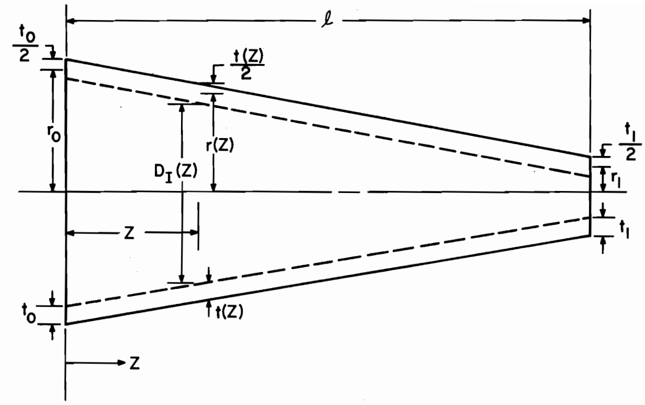

Fig. 3 Model of Conical Section for Transfer Matrix Analysis

integrals in equations (25–28). The error introduced as a result of this assumption is shown below to be generally very small. The expression for the cross-sectional area, $A(z)$, of the conical section is exact for any general conical section (including the case in which the inside and outside surfaces are not parallel). Thus, the evaluation of the integral for the shear term in equation (27) is exact. The expressions presented below for the mass and transverse and polar mass-moments of inertia of a conical section are also exact for any general conical section.

The cross-sectional moment of inertia, $I(z)$, for a hollow circular section is given by

$$I(z) = \frac{\pi}{64}\left(D_0^4(z) - D_I^4(z)\right) = \pi r^3(z)t(z)\left[1 + {}^1/_4\left(\frac{t(z)}{r(z)}\right)^2\right] \quad (29)$$

where $D_0(z)$ is the outside diameter at z; $D_I(z)$ is the inside diameter at z; $r(z)$ is the average radius at z; and $t(z)$ is the wall thickness at z. These parameters, shown in Fig. 3, are related by

$$r(z) = {}^1/_4(D_0(z) + D_I(z)) \quad (30) \text{ and}$$

$$t(z) = {}^1/_2(D_0(z) - D_I(z)) \quad (31)$$

Assuming that t is "small" compared to r, and that t is not a function of z, equation (29) reduces to

$$I(z) = \pi r^3(z)t \quad (32)$$

which is equivalent to the typical "thin-walled" approximation for the cross-sectional inertia of tubes. The error induced by the thin-walled approximation is given by

$$\%\text{Error} = {}^1/_4\left(\frac{t}{r(z)}\right)^2 \times 100 \quad (33)$$

From equation (33), it can be seen that this error for the case of a wall thickness equal to one-third of the average radius (not a very thin wall) is less than three percent. In most practical cases, the wall thickness (and thus the induced error) is substantially less than this. If desired, the expressions obtained from equations (25–28) using this approximation could be modified by "fudge" factors to compensate for this error. However, as these factors would have to be functions of $(t/r(z))$ and these particular errors are generally very small, the addition of these factors is not warranted.

For the case of a conical section, $r(z)$ is given by the function

$$r(z) = r_0 + (r_1 - r_0)z/l = r_0(1 + \rho z/l) \quad (34)$$

where r_0 is the average radius (average of inside and outside radii) at the "left" end of the shaft section; r_1 is the average radius at the "right" end of the shaft section; l is the length of the shaft section; the analysis of the shaft section is performed from left to right; and ρ is a dimensionless constant defined by

$$\rho = (r_1 - r_0)/r_0 \quad (35)$$

Substituting equation (34) into equation (32) results in an expression for cross-sectional area moment of inertia for a conical section given by

$$I(z) = I_0(1 + \rho z/l)^3 \quad (36)$$

where the wall thickness, t, is the average value for the shaft section and

$$I_0 = \pi r_0^3 t \quad (37)$$

For this conical section analysis, the values of E, G and α are assumed to be constant. Thus, I and A become the only parameters in equations (25–28) which remain a function of z.

Substituting equation (36) into equation (25) results in the expression

$$k_1 = \frac{1}{EI_0}\int_0^l \frac{dz}{(1+\rho z/l)^3} \quad (38)$$

where a (in equation (25)) is set equal to zero, since the integrand has no singularities in the region from zero to l. Performing the integration in equation (38) gives

$$k_1 = \left(\frac{l}{2EI_0}\right)(2 + \rho)/(1 + \rho)^2 \quad (39)$$

Substituting equation (36) into equation (26) results in

$$k_2 = \frac{1}{EI_0}\int_0^l \frac{zdz}{(1+\rho z/l)^3} \quad (40)$$

where a is again set equal to zero. Performing the integration in equation (40) gives

$$k_2 = \left(\frac{l^2}{2EI_0}\right)\left(\frac{1}{1 + \rho}\right)^2 \quad (41)$$

Substituting equation (36) into equation (28) results in

$$k_4 = \frac{1}{EI_1}\int_0^l\int_0^{z'} \frac{dzdz'}{(1+\rho z/l)^3} \quad (42)$$

Performing the inside integration gives

$$k_4 = \frac{l}{2EI_0\rho}\int_0^l \left[1 - \frac{1}{(1+\rho z'/l)^2}\right]dz' \quad (43)$$

Evaluating the outside integral gives

$$k_4 = \left(\frac{l^2}{2EI_0}\right)\left(\frac{1}{1 + \rho}\right) \quad (44)$$

The two integrals in equation (27) may be evaluated separately. These integrals are referred to as k_5 and k_6 such that

$$k_5 = \frac{1}{E}\int_0^l\int_0^{z'} \frac{zdzdz'}{I(z)} \quad (45)$$

$$k_6 = \frac{1}{\alpha G}\int_0^l \frac{dz}{A(z)} \quad (46)$$

$$k_3 = k_5 - k_6 \quad (47)$$

Substituting equation (36) into equation (45) results in

$$k_5 = \frac{1}{EI_0}\int_0^l\int_0^{z'} \frac{zdzdz'}{(1+\rho z/l)^3} \quad (48)$$

Performing the inside integration gives

$$k_5 = \frac{l^3}{2EI_0\rho^2}\int_0^l \left[\frac{1}{(1+\rho z'/l)^2} - \frac{z'}{(1+\rho z'/l)} + 1\right]dz' \quad (49)$$

Evaluating the outside integral gives

$$k_5 = \left(\frac{l^3}{2EI_0\rho^3}\right)\left[\frac{\rho(2+\rho)}{(1+\rho)} - 2\ln(1+\rho)\right] \quad (50)$$

The cross-sectional area, $A(z)$, for a hollow circular section is given by

$$A(z) = \frac{\pi}{4}(D_0^2(z) - D_I^2(z)) = 2\pi r(z)t(z) \quad (51)$$

where the parameters have the same meanings as in equation (29).

Equation (31) for $t(z)$ for a conical section may be rewritten as

$$t(z) = t_0 + (t_1 - t_0)z/l = t_0(1 + \tau z/l) \quad (52)$$

where t_0 is the wall thickness at the left end of the shaft section; t_1 is the wall thickness at the right end of the shaft section; and τ is a dimensionless constant defined by

$$\tau = (t_1 - t_0)/t_0 \quad (53)$$

An expression for $r(z)$ is given by equation (34). The cross-sectional area of a conical section is then given by

$$A(z) = A_0(1 + \rho z/l)\,(1 + \tau z/l) \quad (54)$$

where A_0 is the area at the left end of the shaft section, which is given by

$$A_0 = 2\pi r_0 t_0 \quad (55)$$

Substituting equation (54) into equation (46) results in the expression

$$k_6 = \frac{1}{\alpha G A_0}\int_0^l \frac{dz}{(1+\rho z/l)\,(1+\tau z/l)} \quad (56)$$

which involves no simplifying assumptions. Evaluation of the integral in equation (56), after performing a partial fraction expansion, gives

$$k_6 = \left(\frac{l}{\alpha G A_0}\right)\left(\frac{1}{\rho - \tau}\right)\ln\left(\frac{1+\rho}{1+\tau}\right) \quad (57)$$

Equations (50) and (57) are substituted into equation (47) to give

$$k_3 = \left(\frac{l^3}{2EI_0\rho^3}\right)\left[\frac{\rho(2+\rho)}{(1+\rho)} - 2\ln(1+\rho)\right] - \left(\frac{l}{\alpha G A_0}\right)\left(\frac{1}{\rho - \tau}\right)\ln\left(\frac{1+\rho}{1+\tau}\right) \quad (58)$$

Clearly, equations (38), (41) and (44) reduce to the terms in equation (13) for a cylindrical shaft section (ρ equal to zero). However, equation (58), in its present form, becomes indeterminate for a cylindrical shaft section. This equation also becomes indeterminate for the case when ρ is equal to τ. However, the likelihood of ρ being exactly equal to τ is remote and can, in any case, be handled by making a small change in the value of one of these parameters. Note that τ equal to zero represents a conical section of constant wall thickness which is a perfectly legitimate (and probably the most common) case.

Most transfer matrix analyses consider the mass and polar and transverse mass-moments of inertia of each shaft section to be lumped at the ends of the shaft section. In general, a mass station is located at the left end of each shaft section in the transfer matrix model. The mass, as well as the polar and transverse mass-moments of inertia of each shaft section are calculated. Half of this mass and half of each of these moments of inertia are lumped at each of the adjacent mass stations, for a standard cylindrical shaft section. This is equivalent to lumping the mass and moments of inertia for half of the shaft section at each of the adjacent mass stations. However, for a conical shaft section, the mass and moments of inertia of the two halves of the shaft section are not the same and must be calculated separately.

The mass for the left half of the conical section, m_l, is given by

$$m_l = \int dm = \delta\int_0^{l/2}\int_{a(z)}^{b(z)}\int_0^{2\pi} r'd\theta dr'dz \quad (59)$$

where δ is the density of the shaft material, $a(z)$ and $b(z)$ are given by

$$a(z) = r(z) - t(z)/2 \quad (60)$$

$$b(z) = r(z) + t(z)/2 \quad (61)$$

and $r(z)$ and $t(z)$ are given in equations (34) and (52), respectively. Evaluation of the integrals in equation (59) results in the following expression for the mass of the left half of the conical section,

$$m_l = m_0[1 + {}^1/_4(\rho + \tau) + 1/12(\rho\tau)] \quad (62)$$

where ρ and τ are defined in equations (35) and (53), respectively, and m_0 is given by

$$m_0 = \pi r_0 t_0 \delta l \quad (63)$$

Equations (62) and (63) do not depend on any simplifying assumptions.

It should be noted that the values of ρ, τ, r_0 and t_0 used for the mass and inertia calculations for the conical section need not be the same as those used for the shaft flexibility calculations (although in most cases they are the same). For example, in the case of a built-up shaft section composed of one cone inside another cone, it may be desirable to consider only the inside cone for the shaft flexibility analyses while considering the composite of both cones for the mass and inertia analyses.

The mass of the right half of the conical section, m_r, is found in a similar manner as above from

$$m_r = \int dm = \delta\int_{l/2}^{l}\int_{a(z)}^{b(z)}\int_0^{2\pi} r'd\theta dr'dz \quad (64)$$

The integrals in equation (64) are evaluated to give

$$m_r = m_0\left[1 + \frac{3}{4}(\rho + \tau) + \frac{7}{12}(\rho\tau)\right] \quad (65)$$

The polar moment of inertia of the left half of the conical section, I_{Pl}, is obtained from the expression

$$I_{Pl} = \int r'^2 dm = \delta\int_0^{l/2}\int_{a(z)}^{b(z)}\int_0^{2\pi} r'^3 d\theta dr'dz \quad (66)$$

The integrals in equation (66) are evaluated to give

$$I_{Pl} = I_{P0}\{r_0^2[5(4+\rho)\,(8+4\rho+\rho^2) + \tau(40+40\rho + 15\rho^2 + \rho^3)] + \frac{t_0^2}{4}[5(4+\tau)\,(8+4\tau+\tau^2) + \rho(40+40\tau + 15\tau^2 + \tau^3)]\} \quad (67)$$

where I_{P0} is defined as

$$I_{P0} = (m_0 r_0 t_0)/160 \quad (68)$$

Similarly, the polar moment of inertia of the right half of the conical section, I_{Pr}, is derived from

$$I_{Pr} = \int r'^2 dm = \delta\int_{l/2}^{l}\int_{a(z)}^{b(z)}\int_0^{2\pi} r'^3 d\theta dr'dz \quad (69)$$

Evaluation of the integrals in equation (69) results in

$$I_{Pr} = I_{P0}\{r_0^2[5(32+72\rho+56\rho^2+15\rho^3) + \tau(120+280\rho+225\rho^2 +62\rho^3)] + \frac{t_0^2}{4}[5(32+72\tau+56\tau^2+15\tau^3) + \rho(120+280\tau + 225\tau^2 +62\tau^3)]\} \quad (70)$$

The transverse moment of inertia of the left half of the conical section, I_{Tl}, is obtained from the expression

$$I_{Tl} = \int (r'^2\cos^2\theta + z^2)dm = \delta \int_0^{l/2} \int_{a(z)}^{b(z)} \int_0^{2\pi} (r'^3\cos^2\theta + z^2 r')d\theta dr'dz \quad (71)$$

After evaluating the inside integral, equation (71) can be rearranged to give

$$I_{Tl} = \frac{I_{Pl}}{2} + 2\pi\delta \int_0^{l/2} z^2 \int_{a(z)}^{b(z)} r'dr'dz \quad (72)$$

The remaining integrals are evaluated to give

$$I_{Tl} = \frac{I_{Pl}}{2} + \frac{m_0 l^2}{480}[40 + 15(\rho+\tau) + 6\rho\tau] \quad (73)$$

Similarly, the transverse moment of inertia for the right half of the conical section is derived from

$$I_{Tr} = \int (r'^2\cos^2\theta + (l-z)^2)dm = \delta \int_{l/2}^{l} \int_{a(z)}^{b(z)} \int_0^{2\pi} [r'^3\cos^2\theta+(l-z)^2 r']d\theta dr'dz \quad (74)$$

The integrals in equation (74) may be evaluated to obtain

$$I_{Tr} = \frac{I_{Pr}}{2} + \frac{m_0 l^2}{2400}[200 + 125(\rho+\tau) + 8\rho\tau] \quad (75)$$

Clearly, if either ρ or τ (or both) is equal to zero, equation (62), (65), (67), (70), (73) and (75) reduce to simpler forms. In fact, if both ρ and τ are equal to zero, these equations reduce to the corresponding expressions for a cylindrical shaft section. Note that the transverse moment of inertia for each half of the conical section is taken about an axis through the corresponding end of the shaft section, which is consistent with standard transfer matrix analysis procedures.

For a torsional, or coupled torsional-lateral transfer matrix analysis, of a rotor model with a conical section, it is necessary only to perform a flexibility analysis similar to that described above, but for torsional flexibility. The polar mass moment of inertia is given above (in equations (67) and (70)). The cross-sectional polar moment of inertia, $J(z)$, is equal to twice the transverse cross-sectional moment of inertia, $I(z)$. In this case, ϕ_1, the angle of twist at the right end of the shaft section is given by

$$\phi_1 = T_0 \int_a^{a+l} \frac{dz}{J(z)G(z)} + \phi_0 \quad (76)$$

where T_0 and ϕ_0 are the torque and angle of twist at the left end of the shaft section, respectively. For a shaft section with constant values of G and E, equation (76) may be rewritten as

$$\phi_1 = 2T_0\frac{G}{E}k_1 + \phi_0 \quad (77)$$

where k_1 is defined in equation (25) for a general shaft section and in equation (39) for a conical shaft section.

Thus, by the use of the appropriate equations, as defined above, the modelling of a conical section may be handled directly in a transfer matrix rotordynamic analysis.

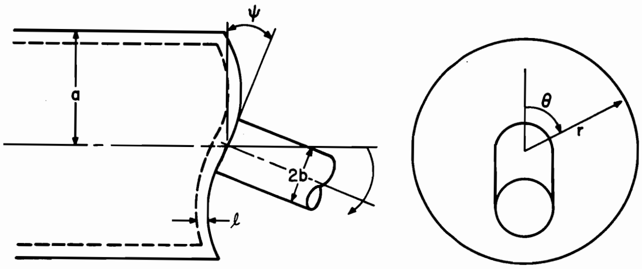

Fig. 4 Model of Trunnion for Transfer Matrix Analysis

Trunnion Analysis

A trunnion is a stepped shaft section with a thin side wall, as shown in Fig. 4. A trunnion, since it is very short, can be considered to be rigid in the radial direction (i.e., $k_3 = k_4 = 0$ in equation (24)). However, it is very flexible in the angular direction when subjected to a bending moment. The trunnion does not deform as a beam and does not, therefore, satisfy equation (1). Instead, the trunnion deforms as a circular disk supported at the edges and satisfies

$$\Delta^4 W(r, \theta) = 0 \quad (78)$$

where ∇ is the del operator in polar coordinates [6] and $W(r, \theta)$ is the axial displacement at the point on the trunnion sidewall with polar coordinates r and θ.

A solution to equation (78) is given by [6]

$$W = (A\rho + B\rho^3 + C\rho^{-1} + F\rho ln\rho)\cos\theta \quad (79)$$

where ln is the natural logarithm, the coefficients A, B, C and F are determined by the boundary conditions, and ρ is a dimensionless quantity defined by

$$\rho = \frac{r}{a} \quad (80)$$

The edge support of the disk may be taken to be either pinned (simply supported) or built-in. In general, the pinned condition should be used for cases in which the sidewall thickness, l, is greater than the wall thickness of the larger adjacent shaft section, t. Similarly, the built-in condition should generally be used when t is greater than l. However, there are instances when this general rule is not valid. For example, the presence of a welded joint between the sidewall and the larger adjacent shaft section may warrant the assumption of a pinned condition, even if t is larger than l. For cases in which t and l are nearly equal, it may be desirable to consider an approximation somewhere between the results of the analyses for the two edge support conditions mentioned above.

For either of these edge support conditions, the expression for W must satisfy the boundary conditions

$$(W)_{\rho=1} = 0 \quad (81)$$

$$\left(\frac{\partial W}{\partial \rho}\right)_{\rho=\beta} = \left(\frac{W}{\rho}\right)_{\rho=\beta}; \ \beta = b/a \quad (82)$$

$$-a \int_{-\pi}^{\pi} (M_r)_{\rho=1}\cos\theta d\theta - a \int_{-\pi}^{\pi} (M_{rt})_{\rho=1}\sin\theta d\theta + a^2 \int_{-\pi}^{\pi} (Q_r)_{\rho=1}\cos\theta d\theta + M = 0 \quad (83)$$

where M is the moment applied to the smaller adjacent shaft section. M_r, M_{rt} and Q_r are the bending and twisting moments and shear force applied to the edge support, given by

$$M_r = -\frac{D}{a^2}\left[\frac{\partial^2 W}{\partial \rho^2} + \mu\left(\frac{1}{\rho}\frac{\partial W}{\partial \rho} + \frac{1}{\rho^2}\frac{\partial^2 W}{\partial \theta^2}\right)\right] \quad (84)$$

$$M_{rt} = (1-\mu)\frac{D}{a^2}\left(\frac{1}{\rho}\frac{\partial^2 W}{\partial r\partial\theta} - \frac{1}{\rho^2}\frac{\partial W}{\partial\theta}\right) \quad (85)$$

$$Q_r = -\frac{D}{a^3}\frac{\partial}{\partial\rho}\left(\frac{\partial^2 W}{\partial\rho^2} + \frac{1}{\rho}\frac{\partial W}{\partial\rho} + \frac{1}{\rho^2}\frac{\partial^2 W}{\partial\theta^2}\right) \quad (86)$$

where μ is Poisson's ratio and D is the "plate stiffness" given by

$$D = El^3/[12(1-\mu^2)] \quad (87)$$

and E is the modulus of elasticity. Equation (82) is based on the assumption that the trunnion sidewall is built-in to the smaller adjacent shaft section.

One additional boundary condition is required, which depends on the edge support. For the case of a pinned edge support, this boundary condition is

$$(M_r)_{\rho=1} = 0 \quad (88)$$

Substituting equation (79) into equations (81), (82), (83) and (88) results in four equations which may be solved for the coefficients, A, B, C, and F, from equation (79). The resulting expression for W is [6]

$$W = \frac{-Ma}{8\pi D[(3+\mu)+(1-\mu)\beta^4]}\{-[(1+\mu) + (1-\mu)\beta^2]\rho^3 + (1+\mu)(1-\beta^2)^2\rho + 2[(3+\mu) + (1-\mu)\beta^4]\rho\ln\rho - \beta^2[(1+\mu)\beta^2 - (3+\mu)]\rho^{-1}\}\cos\theta \quad (89)$$

The angular flexibility, k_A, is given by

$$k_A = \psi/M \quad (90)$$

where ψ, the angle between the two adjacent shaft sections, is derived from

$$\psi = \left(\frac{\partial W}{\partial r}\right)_{r=a} = \frac{1}{a}\left(\frac{\partial W}{\partial\rho}\right)_{\rho=\beta} = \frac{1}{a}\left(\frac{W}{\rho}\right)_{\rho=\beta} \quad (91)$$

Substituting equations (87) and (89) into equation (91), and the result into equation (90) gives

$$k_A = \frac{3(1-\mu^2)}{\pi El^3}\left\{\frac{[2(\beta^2-1) + \mu(\beta^2-1)^2]}{[(3+\mu) + (1-\mu)\beta^4]} - \ln\beta\right\} \quad (92)$$

For the case of a built-in edge support, the fourth boundary condition is

$$\left(\frac{\partial W}{\partial\rho}\right)_{\rho=1} = 0 \quad (93)$$

Substituting equation (93) for equation (88) and performing the procedure described above, results in the following expressions for W and k_A

$$W = \frac{M_a}{8\pi D(\beta^2+1)}[\rho^3+(\beta^2-1)\rho-\beta^2\rho^{-1}-2(\beta^2+1)\rho\ln\rho]\cos\theta \quad (94)$$

$$k_A = \frac{3(1-\mu^2)}{\pi El^3}\left[\frac{(\beta^2-1)}{(\beta^2+1)} - \ln\beta\right] \quad (95)$$

The form in which the trunnion model is included in the transfer matrix analysis is dependent on the orientation of the trunnion in the rotor being analyzed. The angular orientation of the shaft at the right end of the trunnion section (analyzing the rotor from left to right) is

$$\theta_1 = \theta_0 + k_A M \quad (96)$$

where M represents the moment at the small diameter end of the trunnion. If the left end of the trunnion is the small diameter end, M is equivalent to M_0 and

$$\theta_1 = \theta_0 + k_A M_0 \quad (97)$$

Thus, equation (24) is modified such that

$$k_1 = k_A \quad (98)$$ and

$$k_2 = k_3 = k_4 = 0 \quad (99)$$

However, if the right end of the trunnion is the small diameter end, M is equivalent to M_1 and

$$\theta_1 = \theta_0 + k_A M_1 = \theta_0 + k_A M_0 + k_A l V_0 \quad (100)$$

from equation (12). In this case, equation (24) is modified with the substitutions

$$k_1 = k_A \quad (101)$$

$$k_2 = k_A l \quad (102)$$ and

$$k_3 = k_4 = 0 \quad (103)$$

However, since l for a trunnion is generally very small, k_2 in equation (102) may be approximated as being equal to zero. Under this assumption, the orientation of the trunnion does not make any difference.

Thus, a realistic model for a trunnion can be directly represented in a transfer matrix analysis. The mass and polar and transverse moments of inertia for the trunnion sidewall (which are generally very small) are calculated using the equations for a solid cylinder which are used in standard transfer matrix modelling procedures.

Summary and Conclusions

Ordinary transfer matrix analysis modelling procedures do not adequately account for certain unusual rotor section shapes. Two of these shapes which occur frequently are conical sections and trunnions. Direct representation of conical sections and trunnions for transfer matrix analyses provide for increased accuracy and simplicity of the transfer matrix modelling procedures. A framework is also presented upon which an analysis similar to the conical section analysis can be built to take into account any other non-uniform shaft section which may be of interest. This procedure is extended to include the parameters required for torsional, or coupled torsional-lateral, transfer matrix analysis.

The analysis presented for a trunnion is based on a theory of elasticity approach for a circular disk supported at its edge. Since a beam analysis is inappropriate for a trunnion, a standard transfer matrix model of a trunnion is a very inaccurate representation. Consequently, in order to get a reasonable representation of a trunnion, it is necessary to use a modelling procedure such as that presented herein, which takes into account the true mode of deformation of the trunnion.

Acknowledgment

The fourth author wishes to acknowledge support under NSF Grant No. ENG-77-27932, sponsored by the Solid Mechanics Program, Engineering Mechanics Section, Engineering Division of the National Science Foundation.

The first author wishes to acknowledge Mechanical Technology Incorporated, where he was employed when the basis for this paper was first conceived.

References

1 Myklestad, N. O., "A New Method of Calculating Natural Modes of Uncoupled Bending Vibration of Airplane Wings and Other Types of Beams," *Journal of the Aeronautical Sciences*, Apr. 1944, pp. 153–162.

2 Prohl, M. A., "A General Method for Calculating Critical Speeds of Flexible Rotors," ASME, *Journal of Applied Mechanics*, Vol. 12, Vol. 67, 1945, pp. A-142–A-148.

3 Lund, J. W., and Orcott, F. K., "Calculations and Experiments on the Unbalance Response of a Flexible Rotor," ASME, *Journal of Engineering for Industry*, Vol. 89, No. 4, Nov. 1967, pp. 785–796.

4 Lund, J. W., "Stability and Damped Critical Speeds of a Flexible Rotor in Fluid-Film Bearings," ASME, *Journal of Engineering for Industry*, May 1974, pp. 509–517.

5 Walton, J. F. II, *A Preliminary Study on the Effects of Foundation Parameters on Rotor System Critical Speeds*, University of Florida, Oct. 1977, Written under the supervision of J. M. Vance.

6 Timoshenko, S., *Theory of Plates and Shells*, Engineering Societies Monograph, McGraw-Hill Book Company, 1940.